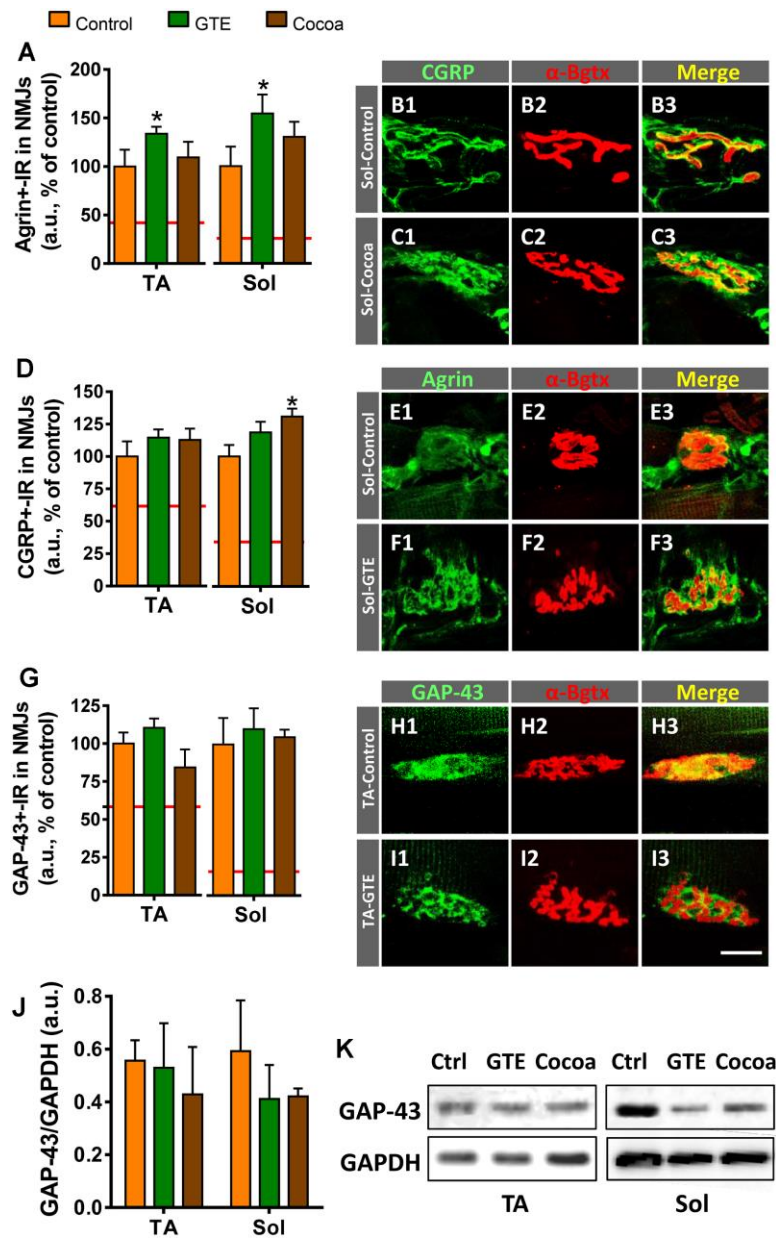
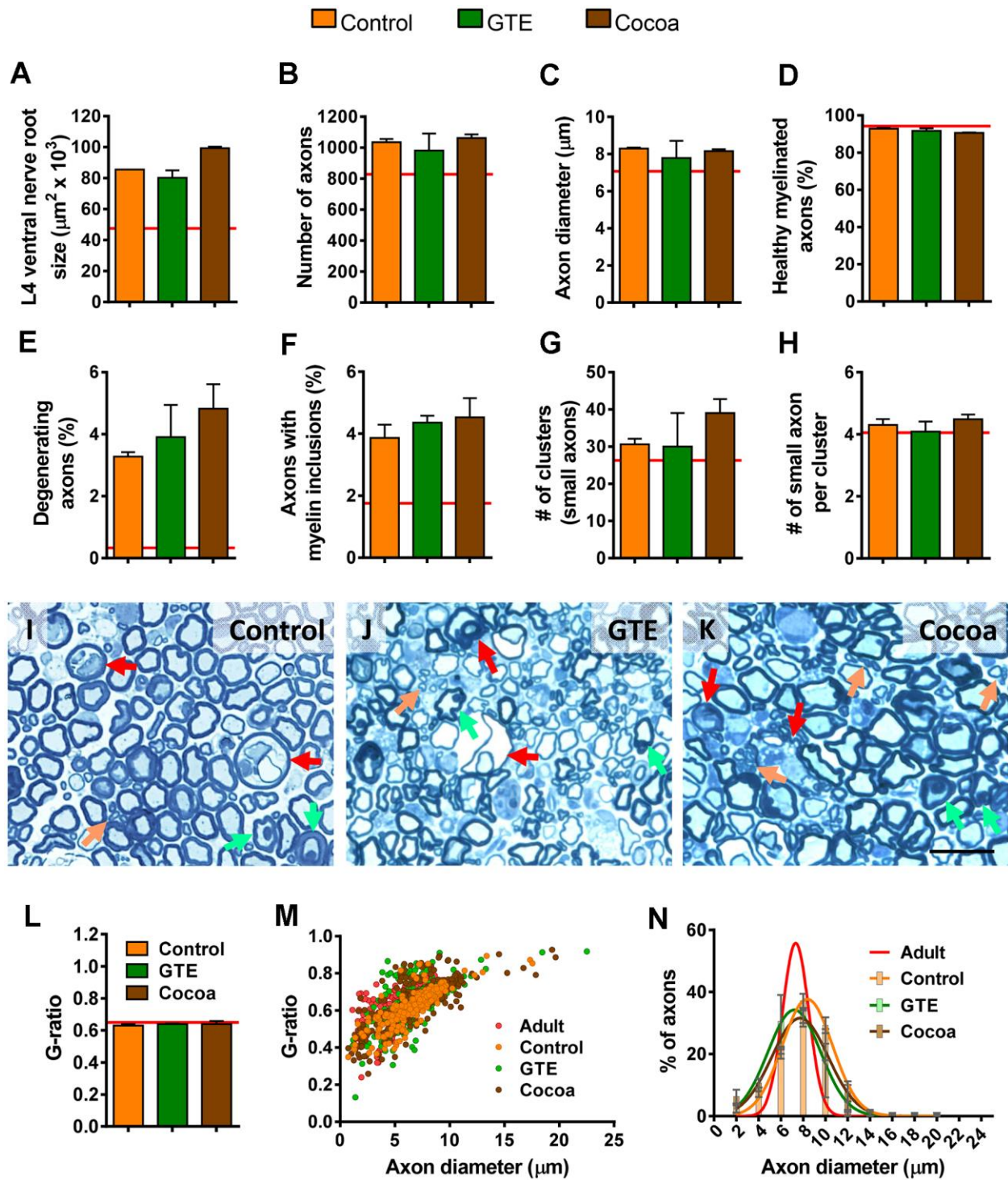


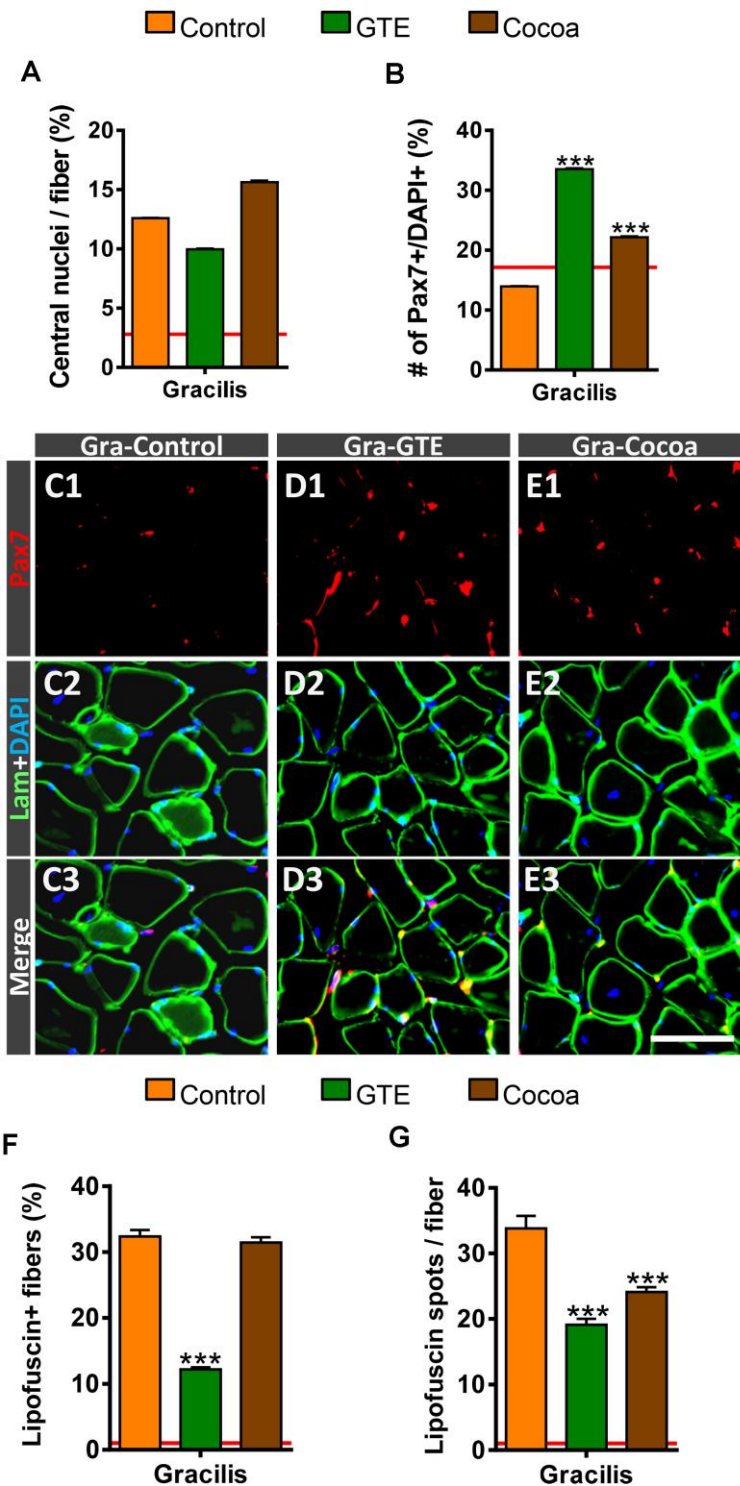
SUPPLEMENTARY FIGURES



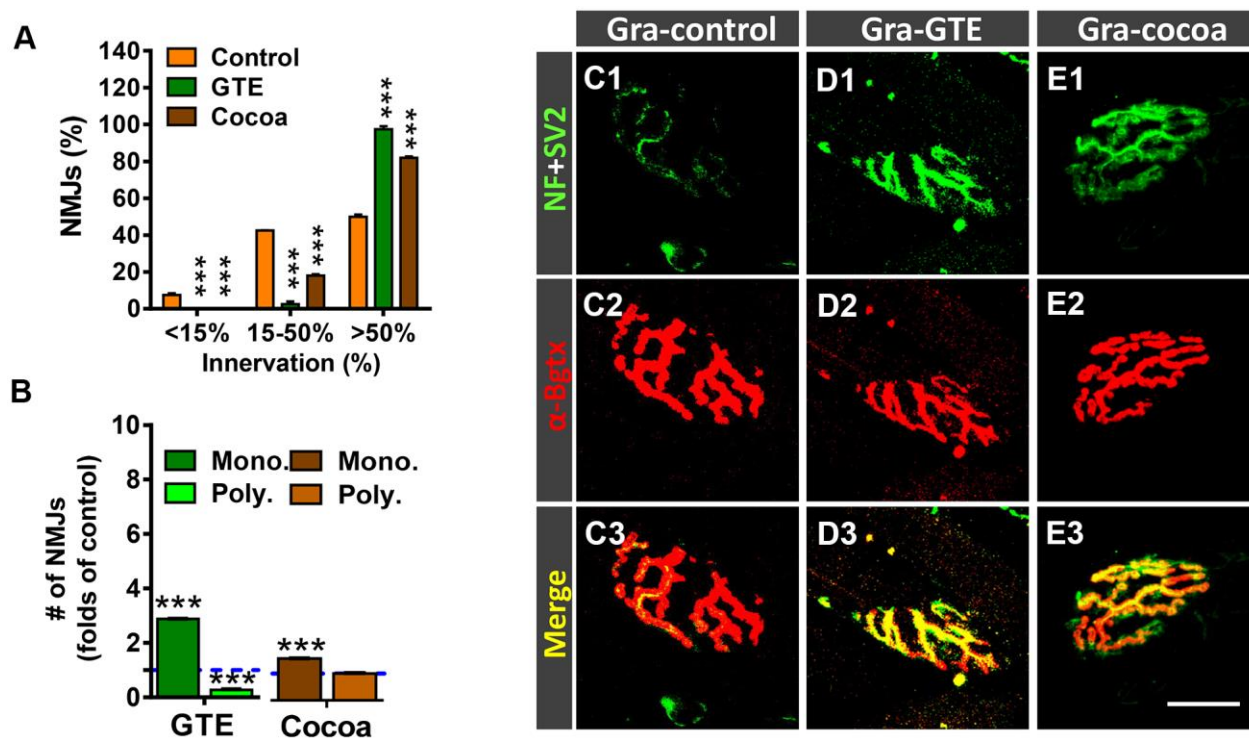
Supplementary Figure 1. Effects of GTE- and cocoa-supplemented diets on CGRP, agrin and GAP-43 expression in NMJs of aged muscles. The quantification of CGRP- (A) agrin- (D) and GAP-43- (G) immunoreactivity (IR, arbitrary units, [a.u.]) in NMJs of TA and Sol muscles from control, GTE and cocoa groups is shown. Data in the graphs are expressed as the mean \pm SEM, and shown as the percentage of change compared with controls; two-way ANOVA, Bonferroni's; *post hoc* test 40-70 NMJs per muscle type were examined; one TA and Sol muscle per animal (3, control; 4 GTE; and 5 cocoa) were used for analysis. (B1–C3, E1–F3, H1–I3) Representative confocal micrographs of NMJs from Sol and TA muscle sections immunolabeled for either, CGRP, agrin or GAP-43 (all in green), as indicated; sections were also stained with α -Bgtx (red) for endplate visualization. Note the slightly, although non-significant increase in agrin-immunoreactivity at NMJs, particularly of Sol muscles, of animals fed with the GTE-supplemented diet. (J) Densitometric analysis of GAP-43 content in TA and Sol muscles of animals belonging to the three experimental groups; data were normalized to GAPDH. Bars represent the values (mean \pm SEM) of 3 mice per condition from 2 independent western blot analysis; two-way ANOVA (Bonferroni's *post hoc* test). (K) Representative western blots of GAP-43 and GAPDH (as loading control) proteins in TA and Sol muscles from mice of control (Ctrl), GTE and cocoa groups. Scale bar in I3 = 20 μ m (valid for B1–C3, E1–F3, H1–I2).



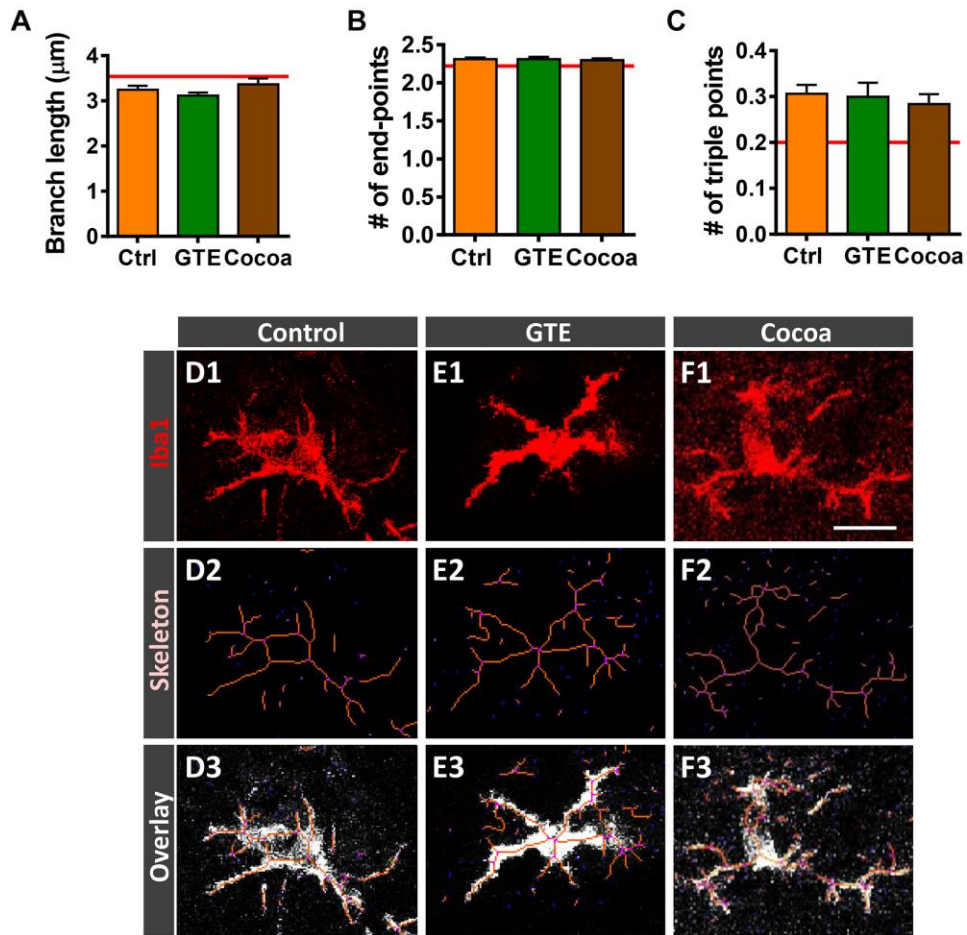
Supplementary Figure 2. Effects of GTE- and cocoa-supplementations in motor axons of aged mice. Analysis was performed in L4 VRs. (A–C) VR size (in μm^2 , [A]), total number of axons (B) and axon diameter (including myelin sheath, in μm , [C]) in VRs. (D–F) Proportion of healthy myelinated axons (D), axons exhibiting a degenerate appearance (E), and those with myelin inclusions (F). (G, H) Number of small ($\leq 6 \mu\text{m}$ diameter) axon clusters (≥ 3 axons) (G) and number of small axons per cluster (H) in VRs. (I–K) Representative images of methylene blue-stained semithin cross-sections of VRs from mice belonging to control (I), GTE (J) and cocoa (K) groups; arrows indicate: degenerating axons (red), axons with myelin inclusions (green) and clusters of small axons (orange). (L, M) Quantification of myelin thickness by *g*-ratio analysis (L) and scatter plot depicting *g*-ratios in relation to axon diameter in (M) VRs. (N) Relative frequency of myelinated axon diameter (in μm); note the slight displacement to left of GTE and cocoa curves, indicative of a diameter reduction of motor axons of animals subjected to dietary flavonoid intake. Data in the graphs are expressed as the mean \pm SEM of 3 VRs from different mice per condition. Scale bar in (K) = 25 μm (valid for [I] and [J]).



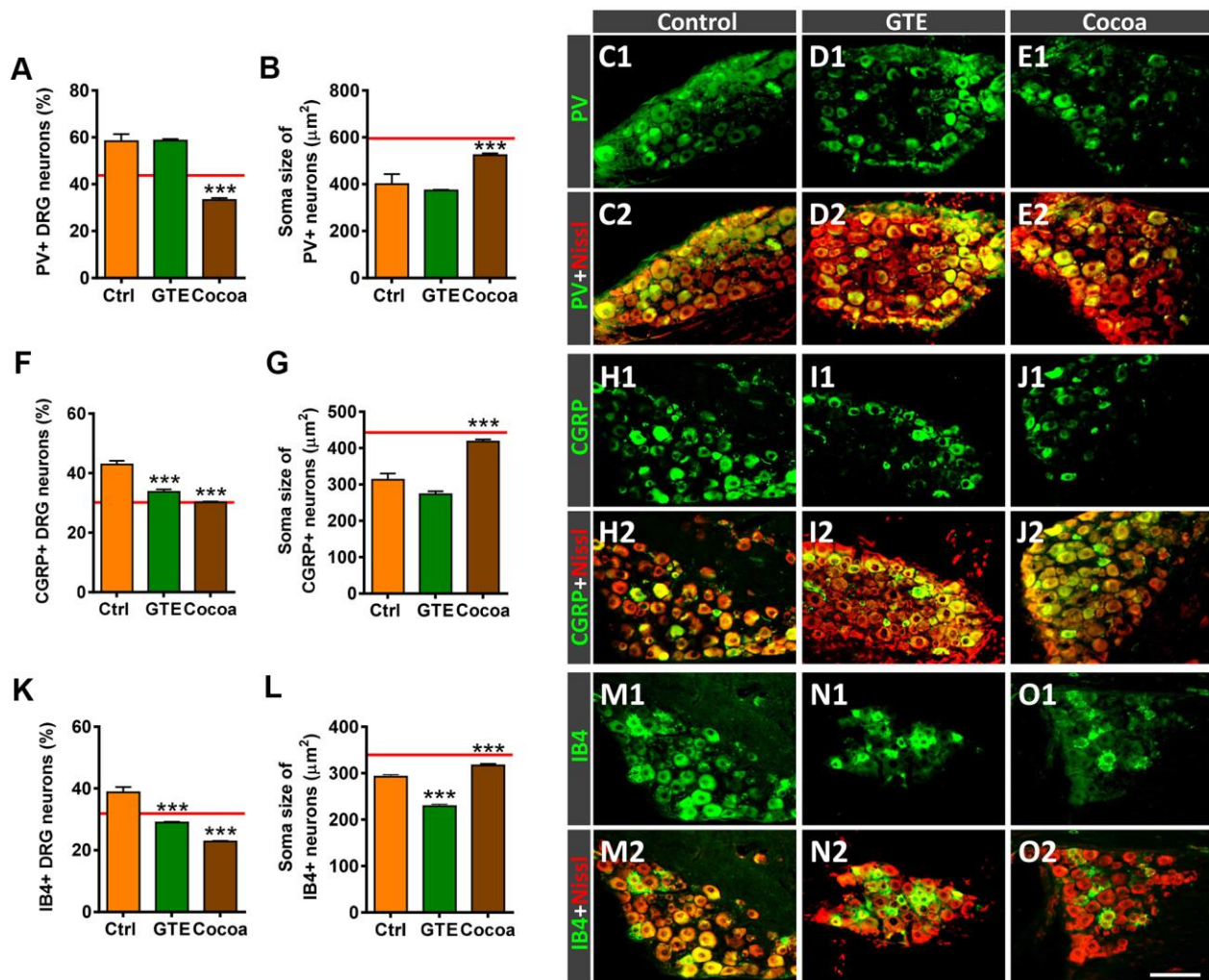
Supplementary Figure 3. Effects of GTE- and cocoa-supplemented diets on aging-associated changes in the proximal hindlimb Gra muscle. (A) Proportion of myofibers displaying central nuclei. (B) Percentage of Pax7-immunostained cells (SCs) with respect to DAPI-positive nuclei. Representative images of a combined immunolabeling for Pax7 (red) and laminin (green), and DAPI staining (blue) in transversal cryosections of Gra muscles from control, GTE and cocoa groups, as indicated. (F, G) Percentage of myofibers containing lipofuscin aggregates (F), and average number of lipofuscin granules per myofiber (G). Data in graphs are expressed as the mean \pm SEM. The average values of different parameters analyzed in adult Gra muscles in a previous study [6] were indicated by a red line in each graph for comparative purposes. *** $p < 0.001$ vs. control (Ctrl), two-way ANOVA, Bonferroni's *post hoc* test; sample size (myofibers): (A) = 1500-2500, (B) = 1700-2200, (F, G) = 1200-1700, from 3-5 mice per condition. Scale bars: 40 μ m in E3 (valid for C1-E2).



Supplementary Figure 4. Changes in the innervation degree of NMJs of Gra muscle in animals fed with GTE- or cocoa-supplemented diets. (A) Proportion of NMJs displaying different degrees of innervation; quantification was based on the percentage of α -Bgtx-labeled postsynaptic site area covered by SV2-immunostained presynaptic terminals (see Materials and Methods, <15% innervation was considered as denervated). (B) Number of NMJs exhibiting single (mono.) or multiple (poly.) innervation expressed as the percentage of control (blue dashed line). (C1–E3) Representative maximal projections of confocal stacks of NMJs from mice of control, GTE and cocoa groups (as indicated in panels); muscle sections were stained with antibodies against NF and SV2 (green, for presynaptic nerve terminals), and α -Bgtx (red, for postsynaptic AChR). Data in graphs are expressed as the mean \pm SEM, *** p < 0.001 vs. control, one or two-way ANOVA, Bonferroni's *post hoc* test; sample size: 40-64 NMJs per muscle from 3-5 animals per condition. Scale bar in (E3) = 20 μ m (valid for C1–E2).

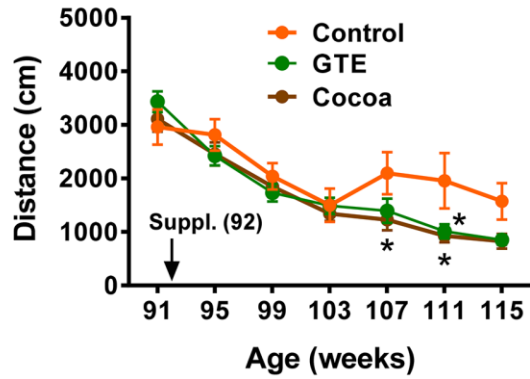
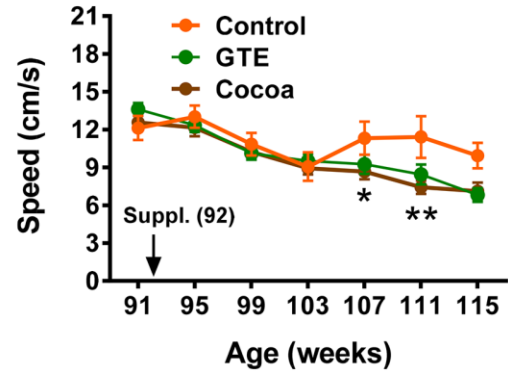


Supplementary Figure 5. Morphometric analysis of microglial complexity by using the skeleton approach (see Materials and Methods). The average branch length (in μm) (A), number of endpoints (B) and triple points (C) are shown in graphs. (D1–F3) Representative images showing Iba1-positive profiles (D1–F1), the skeletonized images (D2–F2), and the overlay of the skeleton and the original image of microglia (D3–F3) in control, GTE and cocoa groups as indicated in panels. Data in the graphs are expressed as the mean \pm SEM; spinal cords of 3 control (Ctrl)-, 4 GTE- and 5 cocoa-group animals were used for analysis; a total of 50-130 images per experimental group were examined; the average values of the different parameters analyzed in adult animals [6] are shown in graphs as a red line for comparison. Scale bar in F1 = 50 μm (valid for D1, E1).



Supplementary Figure 6. Impact of GTE- and cocoa-supplemented diets in age-related changes in DRG sensory neurons.

Proportion (A, F, K) and soma area (in μm^2 , B, G, L) of neurons expressing PV (A, B) or CGRP (F, G), or stained with IB4 (K, L). (C1–E2, H1–J2, M1–O2) Representative micrographs obtained from DRG cryostat sections processed for PV, CGRP and IB4 staining (green) as indicated in panels; sections were also counterstained with fluorescent Nissl (red) for neuron visualization. Data in graphs are expressed as the mean \pm SEM, *** $p < 0.001$ vs. control (Ctrl) (one-way ANOVA, Bonferroni's *post hoc* test); 30-80 images for each condition were analyzed; number of DRG examined: Ctrl = 2, GTE = 3, cocoa = 5 from different animals; the red lines in graphs indicate the mean values in adult mice [6]. Scale bar: in O2 = 100 μm (valid for C1–E2, H1–J2, M1–O1).

A**B**

Supplementary Figure 7. Motor behavior analysis. Motor performance shown as the distance (in cm, **A**) and average speed (cm/s, **B**) assessed by the open-field test in mice from the three groups during the experimental period; the age-related decline in motor performance observed in the animals subjected to the standard (control) diet was not prevented by either GTE or cocoa supplementations; conversely, open-field parameters were even worsened in mice subjected to these dietary supplementations. Data are shown as the mean \pm SEM (number of animals per group: 91 weeks of age, $n = 15$ in all groups; 107 weeks, control $n = 8$, GTE $n = 13$; cocoa $n = 15$; 114 weeks, control $n = 6$, GTE $n = 12$, cocoa $n = 11$); * $p < 0.05$ and ** $p < 0.01$ vs. control; multiple t -test.